Orbital- and k_z-Selective Hybridization of Se 4p and Ti 3d States in the Charge Density Wave Phase of $TiSe_2$

Matthew D. Watson,[1,2,*] Oliver J. Clark,[1] Federico Mazzola,[1] Igor Marković,[1,3] Veronika Sunko,[1,3] Timur K. Kim,[2] Kai Rossnagel,[4,5,6] and Philip D. C. King[1,†]

[1]*SUPA, School of Physics and Astronomy, University of St. Andrews, St. Andrews KY16 9SS, United Kingdom*
[2]*Diamond Light Source, Harwell Campus, Didcot OX11 0DE, United Kingdom*
[3]*Max Planck Institute for Chemical Physics of Solids, Nöthnitzer Straße 40, 01187 Dresden, Germany*
[4]*Institut für Experimentelle und Angewandte Physik, Christian-Albrechts-Universität zu Kiel, 24098 Kiel, Germany*
[5]*Ruprecht-Haensel-Labor, Christian-Albrechts-Universität zu Kiel und Deutsches Elektronen-Synchrotron DESY, 22607 Hamburg, Germany*
[6]*Deutsches Elektronen-Synchrotron DESY, 22607 Hamburg, Germany*

(Received 10 August 2018; published 22 February 2019)

We revisit the enduring problem of the $2 \times 2 \times 2$ charge density wave (CDW) order in $TiSe_2$, utilizing photon energy-dependent angle-resolved photoemission spectroscopy to probe the full three-dimensional high- and low-temperature electronic structure. Our measurements demonstrate how a mismatch of dimensionality between the 3D conduction bands and the quasi-2D valence bands in this system leads to a hybridization that is strongly k_z dependent. While such a momentum-selective coupling can provide the energy gain required to form the CDW, we show how additional "passenger" states remain, which couple only weakly to the CDW and thus dominate the low-energy physics in the ordered phase of $TiSe_2$.

DOI: 10.1103/PhysRevLett.122.076404

Charge density waves (CDWs), typically found in low-dimensional metallic systems, are a striking example of how coupling between the electrons and the crystal lattice can lead to novel ground states. In quasi-1D systems, such as $ZrTe_3$ and organic salts, the CDW phenomenology often closely resembles the famous Peierls instability [1,2]. Transition metal dichalcogenides (TMDCs) such as $NbSe_2$ have become prototypical examples for how CDWs can also occur in quasi-2D metals [3–5]. The starting point for understanding the CDW in the well-known TMDC $TiSe_2$ is, however, an indirect narrow-gap semiconductor. Moreover, the CDW ordering pattern and the normal-state electronic structure are three dimensional [6,7], placing the CDW in $TiSe_2$ far from the conventional picture. Some reports assign $TiSe_2$ as a realization of the long-predicted "exciton insulator" phase, driven purely by electronic interactions [8–14]. The presence of substantial lattice distortions in the ordered phase, however, also points to an important role of electron-phonon coupling, [5,15–18], which may act cooperatively with electron-hole correlations to stabilize the CDW [19–22]. Despite decades of study, the origin and nature of the CDW-like instability in $TiSe_2$ thus remains highly controversial.

In this Letter, we revisit the evolution of the electronic structure of $TiSe_2$ through the CDW transition, paying particular attention to k_z-dependent variations by employing detailed photon-energy dependent ARPES. This allows us to comprehensively determine the positions of the band extrema in this system, identifying a low-temperature band gap that is, surprisingly, smaller than that at high temperatures. We show that this results from a strongly orbital- and k_z-selective hybridization of states involved in the $2 \times 2 \times 2$ CDW, whereby additional "passenger" states which are not strongly hybridized dominate the low energy electronic structure in the ordered phase.

Single crystals were grown by the iodine vapor transport method, and cleaved *in situ* (see Supplemental Material, SM [23]). ARPES measurements were performed at the I05 beam line at Diamond Light Source [24]. We label high-symmetry points of the Brillouin zone according to the notation of the high temperature phase, using the starred Γ^* notation when referring to the $2 \times 2 \times 2$ low-temperature unit cell.

The understanding of the CDW instability in $TiSe_2$ rests upon the details of the normal-state electronic dispersions, and in particular the dimensionality of the relevant bands. Figure 1(a) shows an overview of the occupied states, with a pair of Se $4p_{x,y}$ states forming the low-energy valence bands at the Brillouin zone center, and a Ti 3d–derived conduction band centered at each L point [17,25]. The conduction bands have an elliptical cross section in the k_x-k_y plane, evident in a constant energy map at E_F measured using a photon energy chosen to probe approximately the A-L-H plane [$k_z \approx \pi/c$, Fig. 1(b)]. They are, however, strongly three dimensional. In Figs. 1(e) and 1(g), the ARPES measurements at L points of the Brillouin zone show a clear electronlike conduction band, but the band disperses significantly along k_z such that it is well above E_F at M, in Fig. 1(f). Consistent with the Fermi surface calculated

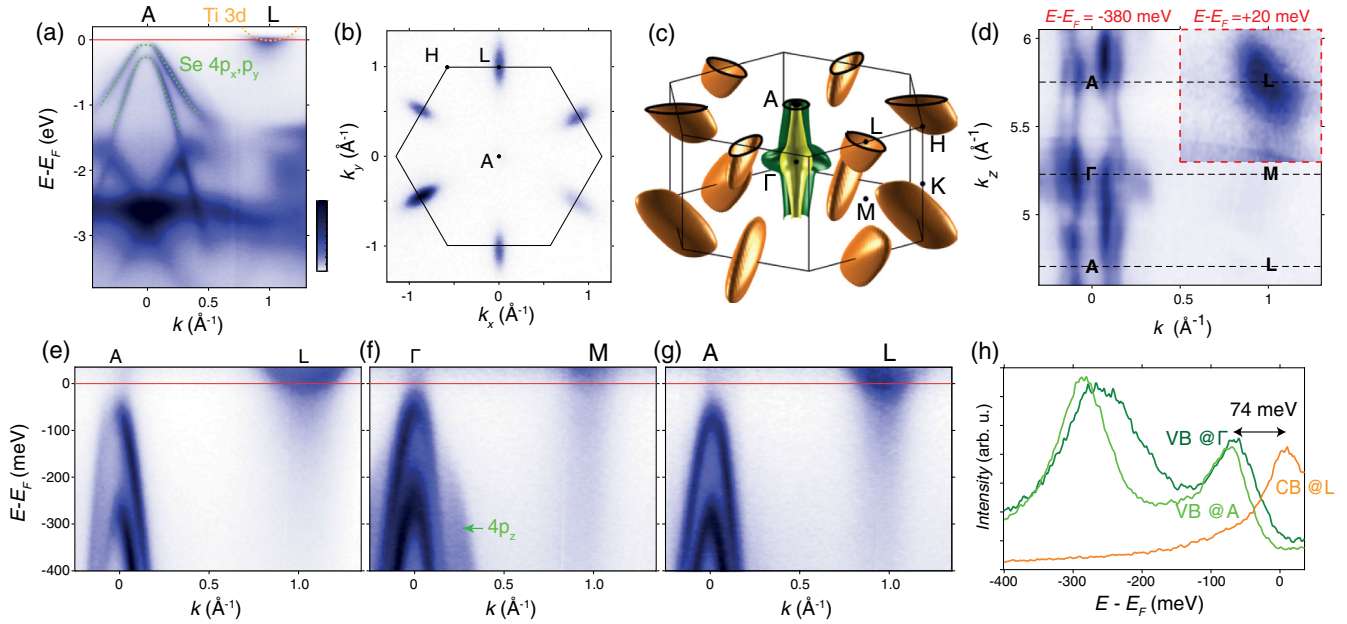

FIG. 1. (a) Valence band dispersion along A-L at $T = 300$ K, measured at a photon energy $h\nu = 121$ eV, in p polarization (p and s polarizations correspond to linear horizontal and linear vertical polarizations, respectively, and the analyzer slit is aligned vertically at the I05 beam line). (b) Constant energy map at E_F (Fermi surface) at $T = 250$ K ($h\nu = 121$ eV, p polarization). (c) Fermi surface of $TiSe_2$ as calculated with a standard DFT code [27]. (d) k_z map, processed from photon-energy dependent data at $E - E_F = -380$ meV. The inset shows the conduction band at $E - E_F = +20$ meV from the same data set. (e)–(g) Dispersions at T = 300 K acquired in s polarization with $h\nu = 44$, 95, and 119 eV, approximately corresponding to L-A-L, M-Γ-M, and L-A-L paths, respectively. (h) Comparison of EDCs at high-symmetry points, indicating an indirect band gap of 74 ± 15 meV. The data in panels (e)–(h) are divided by the Fermi function to reveal the spectral weight above E_F.

from density functional theory (DFT, using the generalized gradient approximation [23]), shown in Fig. 1(c), our photon energy-dependent measurements [Fig. 1(d) [26]] also indicate that this conduction band pocket substantially tilts away from the k_z axis. In contrast, the uppermost valence bands, of Se $4p_{x,y}$ character, are found to be almost 2D; measurements with photon energies chosen to probe the high-symmetry Γ and A points [Figs. 1(e)–1(g)] indicate a k_z dispersion of the upper valence band of < 10 meV [Fig. 1(h)]. A third valence band, of Se $4p_z$ character, appears only around the Γ point and disperses strongly along k_z [Fig. 1(d)]. This band does not play an important role in the CDW ordering and so we do not consider it in detail below.

The normal-state band gap of $TiSe_2$ is a critical parameter, particularly in the context of possible excitonic effects, but previous experimental estimates have varied from a gap of 150 meV to a band overlap of 70 meV [8,25,28–30]. To settle this, in Fig. 1(h) we compare energy distribution curves (EDCs) of the valence bands measured at Γ and A with the conduction band minimum at L. From this, we can confidently estimate the gap between the Γ and L points to be 74 ± 15 meV. Thus in stark contrast to standard DFT calculations which predict a semimetallic state with a large band overlap (SM [23]), the normal state of $TiSe_2$ is a semiconductor with a narrow indirect band gap of 74 ± 15 meV. Crucially, however, this small magnitude of the band gap allows the valence band states to participate in the CDW-like physics by hybridizing with the conduction states.

The mismatched dimensionality of the conduction and valence bands, however, has a major influence on shaping the electronic structure in the ordered state of $TiSe_2$. In Fig. 2(a) we show the normal-state conduction and valence band dispersions along k_z. These are based on the data in Fig. 1, except for the k_z dispersion of the conduction band, for which we use a bandwidth of ~200 meV from DFT calculations. In the CDW phase, the valence and conduction bands hybridize according to an interaction $\Delta_{\mathrm{CDW}}(\mathbf{k})$. While this depends on the microscopics of the interaction terms, a reasonable assumption for $\Delta_{\mathrm{CDW}}(\mathbf{k})$ is a broadly peaked function centered around $\mathbf{q}_{\mathrm{CDW}} = (\pi, 0, \pi) = \mathrm{L}$, where phonon modes are known to soften at the CDW transition of $TiSe_2$ [18,31].

Anticipating the hybridizations allowed by this interaction term, we plot the bands in Fig. 2(a) offset by $\mathbf{q}_{\mathrm{CDW}}$. In this way, the valence band maximum at Γ and the conduction band minimum at L coincide. They can therefore be expected to be strongly hybridized at the CDW transition: as illustrated in Fig. 2(b), the valence bands from Γ and the branch of the conduction band labeled d_2 are significantly repelled from the Fermi level, opening up an energy gap on a scale of $\sim 2\Delta_{\mathrm{CDW}}$. The unoccupied d_2 states are not detectable by ARPES, but are consistent with

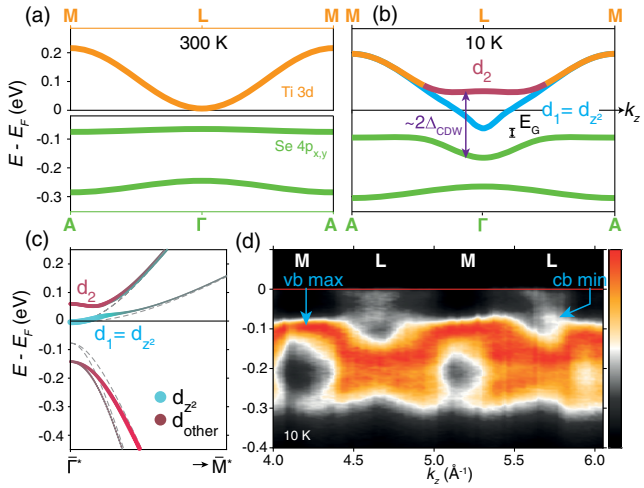

FIG. 2. (a) Schematic k_z dispersions in the normal state. The conduction bands are plotted with a displacement of q_{CDW}. The $4p_z$ valence band is not included. (b) Schematic k_z dispersions in the $3Q$ CDW phase, showing k_z-selective band hybridization. We do not include the backfolded bands. (c) Tight-binding calculations of monolayer $TiSe_2$ showing orbital-selective band hybridization in the CDW phase. Dashed gray lines represent band dispersions at infinitesimal distortion. Color and weight of lines project the difference between the Ti $3d_{z^2}$ character and other $3d$ components (see SM [23] for further plots and details). (d) Experimental k_z dispersion along M-L-M in the CDW phase. The intensity is dominated by bright backfolded valence bands, which display characteristic dips around L points. Conduction pockets are also observed, centered at L points.

interband transitions observed by resonant inelastic x-ray scattering [32]. If these were the only states in the system, this energy scale would also correspond to the low temperature band gap. There are, however, other states to consider.

First, the upper valence band at the A point cannot hybridize significantly with the conduction band states, since the pronounced k_z dispersion of the latter renders it at inaccessibly high energies at M [Figs. 2(a) and 2(b)]. Therefore the dispersion of the valence bands derived from the A point of the high temperature phase will remain largely unchanged through the CDW transition, except for an overall shift of the chemical potential [23]. The band hybridization is thus strongly k_z dependent.

Moreover, the different orbital components of the conduction band couple inequivalently to the CDW order. The $2 \times 2 \times 2$ lattice distortion in $TiSe_2$ is a $3Q$ ordering, corresponding to a superposition of the atomic displacements associated with three softened L-point phonon modes [7]. Thus, electron pockets from three L points are backfolded to the Γ^* point of the reconstructed Brillouin zone [Fig. 3(c)], allowing hybridization with the valence bands. To clarify the form of these hybridizations, we consider a simplified tight-binding analysis for a monolayer of $TiSe_2$ without spin-orbit coupling [19], explained in depth in the SM [23]. We implement a 2×2 CDW by considering only the Ti displacements, and rescaling the Ti-Se d-p hoppings according to the modified bond lengths in the ordered phase. The resulting band dispersions [Fig. 2(c)] show a structure similar to *ab initio* calculations [7,33], where the three backfolded conduction bands split into a doublet (d_2) and singlet (d_1) branch at $\bar{\Gamma}^*$. The valence bands hybridize strongly only with the d_2 branch, while the d_1 branch remains unhybridized and is not pushed away from the Fermi level. Orbital projections reveal that this dichotomy is due to an orbital selectivity of the hybridization, with the unhybridized d_1 branch corresponding exactly to the d_{z^2} orbital projection of the conduction bands, as defined in the crystalographic reference frame. Since the atomic displacements are in plane only [6], the extra hybridization terms associated with the CDW distortion cancel at $\bar{\Gamma}^*$ for the d_{z^2} orbital. A similar orbital selectivity should occur for bulk $TiSe_2$: as well as the k_z selectivity of the d_2-branch hybridization introduced above, an additional unhybridized d_1 branch will remain, shown schematically in Fig. 2(b).

To verify the above considerations, we search for two indicative spectroscopic signatures. The first is that the upper valence band at low temperatures should show characteristic dips along k_z, which can be approximately considered as the inverse profile of the interaction $\Delta_{\mathrm{CDW}}(k_z)$. Such dips are evident in measurements of the k_z dispersion of the bright backfolded valence bands along M-L-M in the low-temperature phase [$T = 10$ K, Fig. 2(d)], very similar to the schematic in Fig. 2(b). The uppermost valence band dips by $\Delta_{\mathrm{CDW}} \approx 100$ meV around L points, where primarily the strongly hybridized valence bands derived from Γ are being observed, but recovers at M points where the more weakly hybridized valence bands derived from the A point are observed, confirming k_z-selective hybridization.

Second, we consider the relative spectral weight of bands that are backfolded by the periodic lattice distortion. As evident in Fig. 3(a), low-temperature measurements show prominent backfolding of valence bands at the L point. This is a famous feature of ARPES spectra in the CDW phase of $TiSe_2$ [5,8,10,17,25,30,34,35], where the backfolded intensity is comparable with the original valence bands at the Γ point, indicating a strong involvement of these states in the CDW. In contrast, the conduction band appears brightly at the L point, but backfolded copies of this band are not clearly apparent in the spectra measured at Γ, consistent with previous reports [8,36]. In fact, careful measurements at the Γ point (see Fig. SM1 in the SM [23]) do reveal a replica of the conduction band, but with extremely weak spectral weight, showing a striking asymmetry with the remarkably bright intensity of the backfolded valence bands. This is entirely consistent with the assignment of the occupied electron band in the low-temperature phase as the branch with d_{z^2} orbital character which remains unhybridized, since it hardly couples to the new periodicity and is thus only very weakly backfolded.

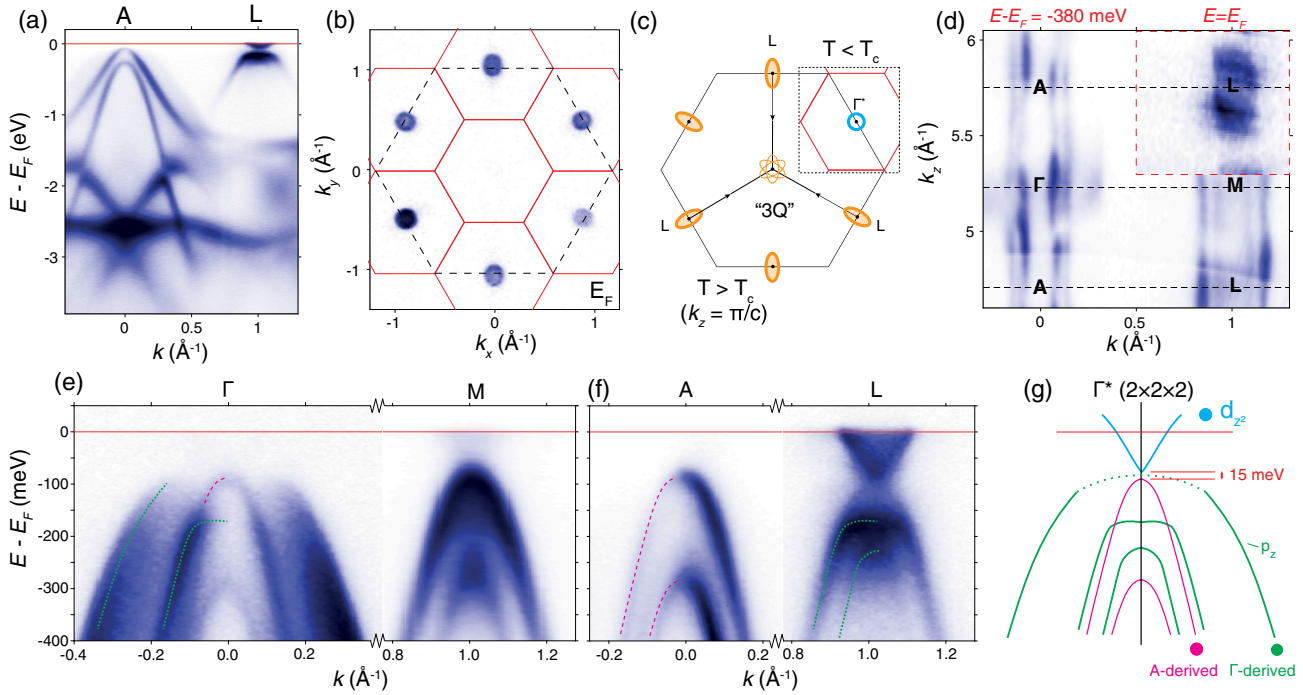

FIG. 3. (a) Valence band dispersion along A-L at 10 K ($h\nu = 121$ eV, p polarization). (b) Fermi surface map, showing near-circular pockets at the L points. (c) In-plane construction of the $3Q$ ordered phase; backfolded bands are dashed, the reconstructed low-temperature Fermi surface is shown inset. (d) Low-temperature k_z map, equivalent to Fig. 1(d), now showing backfolded valence bands, and the Fermi surface in the inset (top right). (e),(f) High symmetry dispersions along Γ-M (31, 100 eV) and A-L (44, 121 eV, all s polarization), respectively. (g) Schematic band structure at Γ^* of the $2 \times 2 \times 2$ Brillouin zone, with an estimated band gap of ∼15 meV.

The measurements and analysis above thus demonstrate that the low-energy physics in the ordered state of $TiSe_2$ is actually dominated by states which do not couple strongly to the CDW. $TiSe_2$ crystals typically exhibit a slight unintentional n doping [6,17,37,38]. Despite the large band shifts associated with the CDW, $TiSe_2$ therefore retains a well-defined ungapped Fermi surface at low temperature [Fig. 3(b)], derived from the unhybridized d_1 branch. Despite the weak coupling of the states which form this Fermi surface to the periodic lattice distortion, they must still respect the symmetry of the low-temperature phase, where Γ, M, A, and L points all become formally equivalent to Γ^* of the $2 \times 2 \times 2$ Brillouin zone. The low temperature conduction band must adhere to $\bar{3}$ symmetry, explaining their almost circular in-plane dispersion observed experimentally, in contrast to the twofold-symmetric elliptical pockets in the high-temperature phase [Figs. 3(b) and 3(c)]. Moreover, the slanting of the Fermi pockets away from the k_z axis seen in the high-temperature phase [Figs. 1(c) and 1(d)] is forbidden at low temperatures [Fig. 3(d)]. The conduction bands also develop a steeper dispersion at low temperatures, consistent with recent first-principles calculations [33].

There are five low-energy valence bands centered at each Γ^* point: three derived from the high-temperature Γ point (one of which is the p_z state) and two derived from the A point [7]. These cannot all be observed simultaneously in one geometry, since the spectral weight as seen by ARPES typically follows the projection of the states onto the high-temperature zone [5]. However, by combining the dispersions observed at different photon energies in Figs. 3(e) and 3(f), we can identify all five, represented schematically in Fig. 3(g). The upper valence band derived from the Γ point is flattened and hybridizes so strongly that in fact it is more clearly observed backfolded at the L point in Fig. 3(f). In contrast, due to the k_z-selective hybridization, the A-point dispersion in Fig. 3(f) is very similar to the equivalent measurement at high temperature [Fig. 1(e)] except that the bands are sharper and there is an overall shift of the chemical potential.

Our measurements in Figs. 3(e)–3(g) allow us to estimate a low-temperature band gap of only ∼15 meV—much smaller than the 74 meV band gap at high temperatures [39]. This is surprising, since second-order electronic phase transitions typically involve opening up or increasing energy gaps, but the ideas of k_z- and orbital-selective hybridizations give insight. The strongly hybridized states, originating from the Γ and L points, are shifted away from E_F by $\pm\Delta_{\mathrm{CDW}} \sim 100$ meV, a large energy scale consistent with the high $T_c \approx 200$ K. However, the band gap in the CDW phase is between two other low-energy states: the A-derived valence band and the unhybridized Ti-d_{z^2} conduction band branch. The energy gap between these passenger states is decoupled from the main hybridization

that drives the CDW, and is, therefore, not required to increase in the CDW phase. The decreased gap between these states at low temperatures compared with the normal state remains a little enigmatic. We speculate that a modified out-of-plane hopping of the d_{z^2} passenger-state conduction band may play a role, as well as other possible many-particle effects [23]. In any case, the key concept is that the overall band gap in the CDW phase is essentially decoupled from the strength of the ordering.

The observation of a smaller band gap in the ordered phase is not easy to reconcile with a purely excitonic mechanism for the phase transition. Moreover, we have observed an ungapped Fermi surface and a near continuum of single particle excitations across the energy scale of $\pm\Delta_{\mathrm{CDW}}$; the existence of these low-energy passenger states would presumably promote the decay of excitons. Nevertheless, the relatively low free carrier density from these passenger states may be insufficient to completely screen the Coulomb interaction between electrons and holes [20], allowing for excitonic correlations to still play an assistive role in the CDW ordering [19–22,40]. Irrespective of the precise microscopic origin of the instability, its underlying driving force is an electronic energy gain from band hybridization. Our measurements highlight how momentum and orbital selectivity can act to decouple such energy gain from the low-energy physics of the ordered state. This is of crucial importance for understanding not only the enigmatic CDW state in $TiSe_2$, but also charge ordering instabilities in multiorbital systems in general.

The research data supporting this publication can be accessed at Ref. [41].

We thank Andrew Hunter, Deepnarayan Biswas, Akhil Rajan, Kaycee Underwood, Kerstin Hanff, and Moritz Hoesch for technical support and useful discussions. We thank Diamond Light Source for access to Beamline I05 (Proposals No. SI19771-1, No. NT18555-1, and No. SI16262-1) that contributed to the results presented here. We gratefully acknowledge support from The Leverhulme Trust (Grants No. RL-2016-006 and No. PLP-2015-144) and The Royal Society. V. S. and O. J. C. acknowledge EPSRC for PhD studentship support through Grants No. EP/L015110/1 and No. EP/K503162/1. I. M. acknowledges PhD studentship support from the IMPRS for the Chemistry and Physics of Quantum Materials.

*mdw5@st-andrews.ac.uk
†philip.king@st-andrews.ac.uk

[1] M. Hoesch, A. Bosak, D. Chernyshov, H. Berger, and M. Krisch, Giant Kohn Anomaly and the Phase Transition in Charge Density Wave $ZrTe_3$, Phys. Rev. Lett. **102**, 086402 (2009).

[2] J.-P. Pouget, The Peierls instability and charge density wave in one-dimensional electronic conductors, C.R. Phys. **17**, 332 (2016).

[3] M. D. Johannes and I. I. Mazin, Fermi surface nesting and the origin of charge density waves in metals, Phys. Rev. B **77**, 165135 (2008).

[4] S. V. Borisenko, A. A. Kordyuk, V. B. Zabolotnyy, D. S. Inosov, D. Evtushinsky, B. Büchner, A. N. Yaresko, A. Varykhalov, R. Follath, W. Eberhardt, L. Patthey, and H. Berger, Two Energy Gaps and Fermi-Surface "Arcs" in $NbSe_2$, Phys. Rev. Lett. **102**, 166402 (2009).

[5] K. Rossnagel, On the origin of charge-density waves in select layered transition-metal dichalcogenides, J. Phys. Condens. Matter **23**, 213001 (2011).

[6] F. J. Di Salvo, D. E. Moncton, and J. V. Waszczak, Electronic properties and superlattice formation in the semimetal $TiSe_2$, Phys. Rev. B **14**, 4321 (1976).

[7] R. Bianco, M. Calandra, and F. Mauri, Electronic and vibrational properties of $TiSe_2$ in the charge-density-wave phase from first principles, Phys. Rev. B **92**, 094107 (2015).

[8] H. Cercellier, C. Monney, F. Clerc, C. Battaglia, L. Despont, M. G. Garnier, H. Beck, P. Aebi, L. Patthey, H. Berger, and L. Forró, Evidence for an Excitonic Insulator Phase in 1T-$TiSe_2$, Phys. Rev. Lett. **99**, 146403 (2007).

[9] M. Cazzaniga, H. Cercellier, M. Holzmann, C. Monney, P. Aebi, G. Onida, and V. Olevano, *Ab initio* many-body effects in $TiSe_2$: A possible excitonic insulator scenario from GW band-shape renormalization, Phys. Rev. B **85**, 195111 (2012).

[10] C. Monney, E. F. Schwier, M. G. Garnier, N. Mariotti, C. Didiot, H. Beck, P. Aebi, H. Cercellier, J. Marcus, C. Battaglia, H. Berger, and A. N. Titov, Temperature-dependent photoemission on 1T-$TiSe_2$: Interpretation within the exciton condensate phase model, Phys. Rev. B **81**, 155104 (2010).

[11] C. Monney, C. Battaglia, H. Cercellier, P. Aebi, and H. Beck, Exciton Condensation Driving the Periodic Lattice Distortion of $1T-TiSe_2$, Phys. Rev. Lett. **106**, 106404 (2011).

[12] S. Hellmann, T. Rohwer, M. Kalläne, K. Hanff, C. Sohrt, A. Stange, A. Carr, M. M. Murnane, H. C. Kapteyn, L. Kipp, M. Bauer, and K. Rossnagel, Time-domain classification of charge-density-wave insulators, Nat. Commun. **3**, 1069 (2012).

[13] C. Monney, G. Monney, P. Aebi, and H. Beck, Electron-hole instability in 1T-$TiSe_2$, New J. Phys. **14**, 075026 (2012).

[14] A. Kogar, M. S. Rak, S. Vig, A. A. Husain, F. Flicker, Y. Il Joe, L. Venema, G. J. MacDougall, T. C. Chiang, E. Fradkin, J. van Wezel, and P. Abbamonte, Signatures of exciton condensation in a transition metal dichalcogenide, Science **358**, 1314 (2017).

[15] Y. Yoshida and K. Motizuki, Electron lattice interaction and lattice instability of 1T-$TiSe_2$, J. Phys. Soc. Jpn. **49**, 898 (1980).

[16] N. Suzuki, A. Yamamoto, and K. Motizuki, Microscopic theory of the CDW state of 1T-TiSe2, J. Phys. Soc. Jpn. **54**, 4668 (1985).

[17] K. Rossnagel, L. Kipp, and M. Skibowski, Charge-density-wave phase transition in 1T-$TiSe_2$ excitonic insulator versus

band-type Jahn-Teller mechanism, Phys. Rev. B **65**, 235101 (2002).

[18] F. Weber, S. Rosenkranz, J.-P. Castellan, R. Osborn, G. Karapetrov, R. Hott, R. Heid, K.-P. Bohnen, and A. Alatas, Electron-Phonon Coupling and the Soft Phonon Mode in $TiSe_2$, Phys. Rev. Lett. **107**, 266401 (2011).

[19] T. Kaneko, Y. Ohta, and S. Yunoki, Exciton-phonon cooperative mechanism of the triple-q charge-density-wave and antiferroelectric electron polarization in $TiSe_2$, Phys. Rev. B **97**, 155131 (2018).

[20] M. Porer, U. Leierseder, J.-M. Ménard, H. Dachraoui, L. Mouchliadis, I. E. Perakis, U. Heinzmann, J. Demsar, K. Rossnagel, and R. Huber, Non-thermal separation of electronic and structural orders in a persisting charge density wave, Nat. Mater. **13**, 857 (2014).

[21] J. van Wezel, P. Nahai-Williamson, and S. S. Saxena, Exciton-phonon-driven charge density wave in $TiSe_2$, Phys. Rev. B **81**, 165109 (2010).

[22] C. Monney, M. Puppin, C. W. Nicholson, M. Hoesch, R. T. Chapman, E. Springate, H. Berger, A. Magrez, C. Cacho, R. Ernstorfer, and M. Wolf, Revealing the role of electrons and phonons in the ultrafast recovery of charge density wave correlations in 1T-$TiSe_2$, Phys. Rev. B **94**, 165165 (2016).

[23] See Supplemental Material at http://link.aps.org/supplemental/10.1103/PhysRevLett.122.076404 for details of the crystal growth and characterization, spectra showing very weak backfolding at the Γ point, tight-binding analysis of the orbital content of the conduction bands, details of the DFT calculation, and further discussion of the low-temperature band gap.

[24] M. Hoesch, T. K. Kim, P. Dudin, H. Wang, S. Scott, P. Harris, S. Patel, M. Matthews, D. Hawkins, S. G. Alcock, T. Richter, J. J. Mudd, M. Basham, L. Pratt, P. Leicester, E. C. Longhi, A. Tamai, and F. Baumberger, A facility for the analysis of the electronic structures of solids and their surfaces by synchrotron radiation photoelectron spectroscopy, Rev. Sci. Instrum. **88**, 013106 (2017).

[25] P. Chen, Y.-H. Chan, X.-Y. Fang, S.-K. Mo, Z. Hussain, A.-V. Fedorov, M. Y. Chou, and T.-C. Chiang, Hidden order and dimensional crossover of the charge density waves in $TiSe_2$, Sci. Rep. **6**, 37910 (2016).

[26] To convert photon energies into k_z, we employ the standard free-electron final state approximation, using an inner potential of 13.5 eV.

[27] P. Blaha, K. Schwarz, G. K. H. Madsen, D. Kvasnicka, J. Luitz, R. Laskowski, F. Tran, and L. D. Marks, *WIEN2k, An Augmented Plane Wave+Local Orbitals Program for Calculating Crystal Properties* (Karlheinz Schwarz, Techn. Universität Wien, Austria, 2018), ISBN: 3-9501031-1-2.

[28] J. C. E. Rasch, T. Stemmler, B. Müller, L. Dudy, and R. Manzke, $1T-TiSe_2$: Semimetal or Semiconductor?, Phys. Rev. Lett. **101**, 237602 (2008).

[29] J. F. Zhao, H. W. Ou, G. Wu, B. P. Xie, Y. Zhang, D. W. Shen, J. Wei, L. X. Yang, J. K. Dong, M. Arita, H. Namatame, M. Taniguchi, X. H. Chen, and D. L. Feng, Evolution of the Electronic Structure of $1T-Cu_xTiSe_2$, Phys. Rev. Lett. **99**, 146401 (2007).

[30] T. E. Kidd, T. Miller, M. Y. Chou, and T.-C. Chiang, Electron-Hole Coupling and the Charge Density Wave Transition in $TiSe_2$, Phys. Rev. Lett. **88**, 226402 (2002).

[31] M. Holt, P. Zschack, H. Hong, M. Y. Chou, and T.-C. Chiang, X-Ray Studies of Phonon Softening in $TiSe_2$, Phys. Rev. Lett. **86**, 3799 (2001).

[32] C. Monney, K. J. Zhou, H. Cercellier, Z. Vydrova, M. G. Garnier, G. Monney, V. N. Strocov, H. Berger, H. Beck, T. Schmitt, and P. Aebi, Mapping of Electron-Hole Excitations in the Charge-Density-Wave System $1T-TiSe_2$ Using Resonant Inelastic X-Ray Scattering, Phys. Rev. Lett. **109**, 047401 (2012).

[33] M. Hellgren, J. Baima, R. Bianco, M. Calandra, F. Mauri, and L. Wirtz, Critical Role of the Exchange Interaction for the Electronic Structure and Charge-Density-Wave Formation in $TiSe_2$, Phys. Rev. Lett. **119**, 176401 (2017).

[34] Th. Pillo, J. Hayoz, H. Berger, F. Lévy, L. Schlapbach, and P. Aebi, Photoemission of bands above the Fermi level: The excitonic insulator phase transition in 1T-$TiSe_2$, Phys. Rev. B **61**, 16213 (2000).

[35] A. Ghafari, L. Petaccia, and C. Janowitz, Splitting of the Ti-3d bands of $TiSe_2$ in the charge-density wave phase, Appl. Surf. Sci. **396**, 1649 (2017).

[36] C. Monney, H. Cercellier, F. Clerc, C. Battaglia, E. F. Schwier, C. Didiot, M. G. Garnier, H. Beck, P. Aebi, H. Berger, L. Forró, and L. Patthey, Spontaneous exciton condensation in 1T-$TiSe_2$: BCS-like approach, Phys. Rev. B **79**, 045116 (2009).

[37] S. H. Huang, G. J. Shu, W. W. Pai, H. L. Liu, and F. C. Chou, Tunable Se vacancy defects and the unconventional charge density wave in $1T-TiSe_{2-\delta}$, Phys. Rev. B **95**, 045310 (2017).

[38] We estimate the carrier density here to be $\approx 3 \times 10^{19}$ cm^{-3}.

[39] In fact 15 meV is an upper limit on the low temperature band gap, since we were unable to pinpoint the exact top of the p_z band dispersion.

[40] H. Watanabe, K. Seki, and S. Yunoki, Charge-density wave induced by combined electron-electron and electron-phonon interactions in $1T-TiSe_2$: A variational Monte Carlo study, Phys. Rev. B **91**, 205135 (2015).

[41] University of St Andrews Research Portal, https://doi.org/10.17630/5c9c3806-d8bf-4540-92c2-118ad69dd281.